PHYSICAL REVIEW B

CONDENSED MATTER

THIRD SERIES, VOLUME 34, NUMBER 11 1 DECEMBER 1986

Low-temperature nuclear-spin relaxation times and line shapes for H_2 in solid nonmagnetic hosts

P. A. Fedders

Department of Physics, Washington University, St. Louis, Missouri 63130

(Received 21 July 1986)

We calculate the nuclear-spin relaxation time T_1 and line-shape function for isolated ortho-($J=1$) H_2 molecules in solid nonmagnetic hosts located at sites with various crystal-field symmetries. This work includes modifications of earlier work so that the formalism can be used in regimes where Γ_m, the molecular angular momentum relaxation rate, is not large compared to the molecular-nuclear spin coupling constants ω_c and ω_d. The formalism also allows for a nonzero value of the quadrupolarization $\langle 3J_z^2-J^2\rangle$. With these changes the theory can be used at temperatures at and below about 4 K where line shapes evolve from Lorentzians into Pake doublets.

I. INTRODUCTION

In earlier work[1,2] we calculated nuclear-spin relaxation times T_1 and T_2 for isolated ortho-H_2 molecules in solid nonmagnetic hosts. This work showed how the relaxation times depend quantitatively and sometimes qualitatively on the magnitude, symmetry, and orientation of the crystal fields experienced by the H_2 molecules. Several apparent anomalies have been explained by using this theory.[3-6] However, the approximation used in this earlier work was that Γ_m, the relaxation or correlation rate of the molecular angular momentum (or spin), was much greater than ω_d and or ω_c, the frequencies which characterize the coupling of the nuclear spin to the angular momentum of the molecule. Since Γ_m depends strongly on the temperature, this approximation is not valid below about 4 K in most materials.

However, there are recent NMR measurements at lower temperatures of apparently isolated H_2 molecules in amorphous Si:H whose spectra that broaden out into a Pake doublet as the temperature decreases.[7] Further, there are elements of the NMR spectra at high concentrations of H_2 that we believe are independent of the concentration and can be examined by our formalism. Thus in this paper we extend our results to lower temperatures by lifting the restriction that Γ_m be larger than ω_d and ω_c. In addition, we allow for a nonzero value of the quadrupolarization $\langle 3J_z^2-J^2\rangle$, where **J** is the angular-momentum operator for the molecule and the angular brackets denote the thermal average. Although some elements of our calculation have been considered by other investigators,[3,8] some important aspects have been left out of their work. In the rest of this section we shall briefly review our model and approximations. The calculations are described in Sec. II and the results are discussed in Sec. III.

Since we will only be considering temperatures well below 100 K, only the $J=1$ state of the ortho-H_2 molecule need be considered.[2] As in Ref. 1, we refer to the molecular angular momentum as molecular spin of magnitude $J=1$ and the two protons will be referred to as a single nuclear spin of magnitude $I=1$. Except for a Zeeman splitting arising from an external magnetic field, the nuclear spins experience the environment of the molecule only indirectly through the molecular spin. The Hamiltonian $H_{\rm int}$ connecting the nuclear- and molecular-spin systems of a single molecule can be written as

$$H_{\rm int}=-\hbar\omega_d\sum_{m=-2}^{m=+2}B_{2,m}A_{2,m}^{\dagger}-\tfrac{2}{3}\hbar\omega_c\sum_{m=-1}^{m=+1}B_{1,m}A_{1,m}^{\dagger}\ , \tag{1}$$

where the $A_{l,m}$ and $B_{l,m}$ are the irreducible multipole operators for the molecular spin J and the nuclear spin I, respectively.

The line shape and relaxation rates of the nuclear spins are determined by the states of the molecular spin and by the fluctuations among these states. The static environment of a molecule is characterized by a set of electric field gradients V_{ij} which, in turn, determine the frequencies of the transitions between the states. Dynamically, an isolated molecule can be characterized by a set of correlation or relaxation rates Γ_{lm} associated with the operators A_{lm}. We shall usually assume that the main relaxation mechanism is due to phonons (or some other independently fluctuating field that generates electric field gradients). If this is the case then[9,10] $\Gamma_{lm}=\Gamma_l$, and $\Gamma_2=0.6\Gamma_1$, since we are dealing with an $I=1$ system. Although our formalism is valid for electric field gradients of any magnitude, our calculations will be limited to the more tractable regimes where each V_{ij} is very large or very small compared to the Γ_l or ω_0, the Larmor frequency of the nuclear spins. Very large field gradients will push the resonant frequencies of some of the molecular-spin nor-

mal modes so high that they will cease to be effective in relaxing the nuclear spins. If the Γ_l arise from phonons, and thus depend on the temperature, the conditions of large or small electric field gradients can also depend on the temperature. For example, isolated H_2 molecules in rare-gas solids and in a-Si:H show[3,11] relaxation rates which are proportional to T^2 at temperatures $T \gg \Theta_D$ (the Debye temperature) and which are proportional to T^7 for $T \ll \Theta_D$. This is the expected temperature dependence for the anharmonic Raman process.[12]

In the rest of this paper we shall consider only the cases of axial symmetry and no symmetry since we believe that sites of higher symmetry are rare or nonexistent in low-temperature solids. Finally, we wish to note that our description of the H_2 molecule has a good deal of validity even for concentrated H_2. This point will be addressed in more detail in Sec. III.

II. CALCULATIONS

A. Axial symmetry

For a given set of electric field gradients there exists a coordinate system where the local axes are the principal axes of the electric field gradients. The axis that has the largest electric field gradient is defined to be the z axis in the crystal coordinate system and the external magnetic field $\mathbf{H}_0$ defines the z axis of the lab system. It is convenient to refer to the nuclear spins in the laboratory frame and to the molecular-spin operators in the crystal coordinate system. Thus, in the rest of this paper all nuclear-spin and molecular-spin operators will be understood to refer to the laboratory and crystal coordinate systems, respectively.

If the largest electric field gradient is large with respect to the Γ_l and ω_0, but the remaining electric field gradients are not, the system is said to possess axial symmetry. As discussed earlier,[1] the normal modes (l,m) with $m=\pm 1$ then have frequencies that are so large that they are totally ineffective in relaxing the nuclear spins. Thus, all operators A_{lm} with $m=\pm 1$ can be ignored. Using the coordinate transform in Ref. 1, one thus obtains

$$\begin{aligned} H_{\rm int} = & -\tfrac{2}{3}\hbar\omega_c A_{1,0}\sum_m a(1,0,m)B_{1,m} \\ & -\hbar\omega_d \sum_m [A_{2,2}a(2,-2,m)B_{2,m} \\ & \quad + A_{2,0}a(2,0,m)B_{2,m} \\ & \quad + A_{2,-2}a(2,2,m)B_{2,m}] , \end{aligned} \tag{2}$$

where the $a(l,m,m')$ are given in Ref. 1.

The calculation for T_1 proceeds almost exactly the same as in Ref. 1. The reason for this is that the effective coupling between the nuclear and molecular spins for processes which change the nuclear magnetization is Ω,

$$\Omega \sim \omega_x^2 \Gamma_1/(\omega_0^2+\Gamma_1^2) , \tag{3}$$

where ω_x is ω_c or ω_d, ω_0 is the Larmor frequency of the nuclear spins, and we use the fact that $\Gamma_1 \sim \Gamma_2$. For the purposes of this paper we shall assume that ω_0 is large enough that $\Omega \ll \Gamma$. Since $\omega_x \sim 10^5$ sec^{-1} and typically $\omega_0 \sim 10^7$–10^9 sec^{-1}, this restriction is essentially always met. Since $\Omega \ll \Gamma$, the effects of the nuclear spin on the molecular spin can be ignored as in Ref. 1. However, in this paper we are considering low enough temperatures or large enough electric field gradients that $\langle A_{20}\rangle \sim \langle (J_z^2-\frac{2}{3})\rangle$ is nonzero. Since the formalism in Ref. 1 makes use[13] of the fact that the thermal average of all of the operators is zero, the appropriate dynamical operator for $l=2$, $m=0$ is $\tilde{A}_{20}$, where

$$\tilde{A}_{20} = A_{20} - \langle A_{20}\rangle , \quad \langle A_{20}\rangle = 3\langle J_z^2 - \tfrac{2}{3}\rangle/2^{1/2} . \tag{4}$$

With this modification the calculation is then similar to that in Ref. 1 and one obtains

$$\begin{aligned} 1/T_1 = & (1+\tfrac{1}{2}a)\{(2\omega_c^2/3)(1-z^2)F_1(\omega_0)+(3\omega_d^2/4)[(1-z)^4F_2(2\omega_0+2\omega_j z)+(1+z)^4F_2(2\omega_0-2\omega_j z) \\ & +(1-z^2)(1-z)^2F_2(\omega_0+2\omega_j z)+(1-z^2)(1+z)^2F_2(\omega_0-2\omega_j z)]\} \\ & +(1+\tfrac{1}{2}a)(1-a)(9\omega_d^2/2)[(1-z^2)^2F_2(2\omega_0)+z^2(1-z^2)F_2(\omega_0)] , \end{aligned} \tag{5}$$

where

$$\begin{aligned} & F_l(\omega) = \Gamma_l/(\omega^2+\Gamma_l^2) , \\ & z = \cos\theta , \\ & a = \langle A_{20}\rangle 2^{1/2} = \langle 3(J_z^2-\tfrac{2}{3})\rangle , \end{aligned} \tag{6}$$

and ω_j is the Larmor frequency of the molecular spin.

In order to solve the line-shape problem, we must treat all terms in $H_{\rm int}$ that conserve m_I and m_J exactly, while the rest of the terms in the Hamiltonian can be calculated perturbatively as in Ref. 1. The reason for this is that these diagonal terms cause changes in the molecular-spin spectrum of order ω_x^2/Γ_1, which is not necessarily small with respect to Γ_1. The remaining off-diagonal terms contribute terms of order Ω as given by Eq. (3). These diagonal terms are those that are proportional to $A_{l0}B_{l'0}$ in Eq. (2). If one forms an equation of motion for B_{11} using this truncated Hamiltonian, one obtains an equation which couples to $A_{10}B_{11}$ and $A_{20}B_{21}$. In fact, this truncated Hamiltonian connects the following six operators: B_{11}, B_{21}, $A_{10}B_{11}$, $A_{10}B_{21}$, $\tilde{A}_{20}B_{11}$, and $\tilde{A}_{20}B_{21}$. These six equations can be written as

$$\sum_{\beta=1}^{6} M_{\alpha\beta}p_\beta = 0 , \tag{7}$$

where the nonzero elements of the 6×6 matrix $M_{\alpha\beta}$ are given in the Appendix by Eqs. (A1) and the operator combinations p_β are given by Eqs. (A2). In these equations

$$a_1 = \tfrac{2}{3}\omega_c z , \quad a_2 = \tfrac{1}{2}\omega_d(3z^2-1) . \tag{8}$$

The decay rates Γ_{a1} and Γ_{a2} are the decay rates arising from the off-diagonal terms which can be treated as perturbations. They are easily seen to be

$$\Gamma_{a1}=(\omega_c^2/3)(1+\tfrac{1}{2}a)(1-z^2)F_1(\omega_0)$$
$$+\omega_d^2(1+\tfrac{1}{2}a)\{\tfrac{27}{8}(1-z^2)^2F_2(2\omega_j z)+\tfrac{3}{4}(1-z^2)[(1-z)^2F_2(\omega_0+2\omega_j z)+(1+z)^2F_2(\omega_0-2\omega_j z)]$$
$$+\tfrac{9}{8}(1-z^2)[(1+z)^2F_2(\omega_0-2\omega_j z)+(1-z)^2F_2(\omega_0+2\omega_j z)]$$
$$+\tfrac{3}{16}[(1+z)^4F_2(2\omega_0-2\omega_j z)+(1-z)^4F_2(2\omega_0+2\omega_j z)]\}$$
$$+\omega_d^2(1+\tfrac{1}{2}a)(1-a)[\tfrac{45}{4}z^2(1-z^2)F_2(\omega_0)+\tfrac{9}{8}(1-z^2)^2F_2(2\omega_0)]\ , \tag{9}$$

$$\Gamma_{a2}=(5\omega_c^2/3)(1+\tfrac{1}{2}a)(1-z^2)F_1(\omega_0)$$
$$+\omega_d^2(1+\tfrac{1}{2}a)\{\tfrac{27}{8}(1-z^2)^2F_2(2\omega_j z)+\tfrac{3}{8}(1-z^2)[(1+z)^2F_2(\omega_0-2\omega_j z)+(1-z)^2F_2(\omega_0+2\omega_j z)]$$
$$+\tfrac{3}{16}[(1+z)^4F_2(2\omega_0-2\omega_j z)+(1-z)^4F_2(2\omega_0+2\omega_j z)]\}$$
$$+\omega_d^2(1+\tfrac{1}{2}a)(1-a)[\tfrac{9}{4}z^2(1-z^2)F_2(\omega_0)+\tfrac{9}{8}(1-z^2)^2F_2(2\omega_0)]\ . \tag{10}$$

If the difference between Γ_{1a} and Γ_{2a} is ignored, the 6×6 matrix equation reduces to two 3×3 matrix equations. This point is discussed further in the Appendix.

B. No symmetry

In the case where the second largest electric field gradient in the principal axis system is greater than Γ_l and ω_0, the system is said to possess no symmetry. In this case, following Sullivan,[13] we let θ and ϕ be the spherical angles of the magnetic field $\mathbf{H}_0$ with respect to this crystal-field system. In terms of our earlier work,[1]

$$r=2\cos^2\phi-1\ . \tag{11}$$

As discussed in Ref. 1, all of the normal modes except two are now pushed to high enough frequencies so that they are ineffective in relaxing the nuclei. The two operators that are left are A_{20} and A_{b0}, where

$$A_{b0}=(A_{2,2}e^{i\phi}+A_{2,-2}e^{-i\phi})/2^{1/2}\ . \tag{12}$$

The part of the Hamiltonian that survives is

$$H_{\rm int}=-\hbar\omega_d\sum_m\{A_{20}a(2,0,m)B_{2m}+A_{b0}[a(2,-2,m)B_{2m}e^{-i\phi}+a(2,-2,m)e^{i\phi}B_{2m}]/2^{1/2}\}\ . \tag{13}$$

The calculations now proceed very much as in the case of axial symmetry. We apply one restriction in assuming that $\langle A_{b0}\rangle=0$. If this restriction is not imposed, the equations become extremely messy. Thus we are limited to describing systems where not more than one splitting is large compared to kT. In this case, T_1 is given by the equation

$$\frac{1}{T_1}=\omega_d^2a_+^2\{6[z^2+\tfrac{1}{4}(z^2-1)\cos^2\phi]F_2(2\omega_0)+\tfrac{3}{2}(1-z^2)[1-(1-z^2)\cos^2\phi]F_2(\omega_0)\}$$
$$+\omega_d^2a_+^2a_-^2[\tfrac{9}{2}(1-z^2)^2F_2(2\omega_0)+\tfrac{9}{2}z^2(1-z^2)F_2(\omega_0)]\ , \tag{14}$$

where

$$a_+^2=1+\tfrac{1}{2}a\ ,\quad a_-^2=1-a\ . \tag{15}$$

The form of the 6×6 matrix corresponding to Eq. (7) has the same form as given by Eq. (A1), except that

$$a_1=\tfrac{3}{2}\omega_d(1-z^2)\cos\phi\ ,\quad a_2=\tfrac{1}{2}\omega_d(3z^2-1)\ . \tag{16}$$

The relevant p_β's are given by Eqs. (A4). Further, Γ_{a1} and Γ_{a2} are given by the equations

$$\Gamma_{a1}=\omega_d^2a_+^2\{\tfrac{3}{2}[z^2+\tfrac{1}{4}(z^2-1)\cos^2\phi]F_2(2\omega_0)+\tfrac{15}{4}[1-(1-z^2)\cos^2\phi]F_2(\omega_0)\}$$
$$+\omega_d^2a_+^2a_-^2[\tfrac{9}{8}(1-z^2)^2F_2(2\omega_0)+\tfrac{45}{4}z^2(1-z^2)F_2(\omega_0)]\ , \tag{17}$$

$$\Gamma_{a2}=\omega_d^2a_+^2\{\tfrac{3}{2}[z^2+\tfrac{1}{4}(z^2-1)\cos^2\phi]F_2(2\omega_0)+\tfrac{3}{4}[1-(1-z^2)\cos^2\phi]F_2(\omega_0)\}$$
$$+\omega_d^2a_+^2a_-^2[\tfrac{9}{8}(1-z^2)^2F_2(2\omega_0)+\tfrac{9}{4}z^2(1-z^2)F_2(\omega_0)]\ . \tag{18}$$

III. RESULTS

In this section we shall present and discuss the results derived in the preceding section. However, we shall first compare our formalism to that of Gaines, Mukherjee, and Shi[5] (hereafter referred to as GMS), who earlier theoretically investigated the NMR line shape of dilute ortho-H_2 and solid para-H_2. They did not calculate T_1 and they neglected the off-diagonal terms leading to Γ_{a1} and Γ_{a2}. However, T_1 is not used in calculating the line shape and Γ_{a1} and Γ_{a2} are unimportant in their regime where $\omega_0 \gg \Gamma_1$. GMS considered two cases: (a) where J_ζ is characterized by the values $+1$, 0, and -1, where J_ζ is the projection of the rotational angular momentum on the crystal axis. This case turns out to be the case that we call axial symmetry. In their case (b) the states of J_ζ are chosen to be

$$|s\rangle=(1/2^{1/2})(|1\rangle+|-1\rangle)\,,$$
$$|a\rangle=(1/2^{1/2})(|1\rangle-|-1\rangle)\,, \qquad (19)$$
$$|0\rangle\,.$$

This turns out to be our case of no symmetry with $\cos\phi=0$. Given the above restrictions, GMS's treatment of the line-shape problem is correct if $\langle A_{20}\rangle=0$. However, their inclusion of low-temperature effects is incomplete. They include the thermal occupation of the m_j states in the weighting of the spectrum, but they do not include the effects of a nonzero $\langle A_{20}\rangle$ on the modes themselves.

Our results are the solution to the 6×6 matrix or two 3×3 matrices contained in the Appendix. The general solution to these equations cannot be expressed in a simpler way. Further, usually one is interested in the line shape averaged over all angles. Our approach will be to present formulas and a discussion from the limiting cases. The trend for a single angle can be fairly well understood from the formulas. Then a number of figures will be presented for the line shape averaged over all angles in the regime between the limiting cases. In all of this we shall assume that $\Gamma_{a1}=\Gamma_{a2}=\Gamma_a$, and in the figures a very small Γ_a is chosen. In fact, Γ_{a1} and Γ_{a2} may be rather unimportant in most cases of interest. However, they must be included to recover the exact results of Ref. 1 in the case where Γ_1 is not much smaller than ω_0. Thus there are two sets of three modes and their spectral weight or relative contribution to the line shape. We shall use the notation of a complex frequency Ω whose real part is the real frequency as measured from the center of the line, ω_0, and whose imaginary part is the decay rate of the mode. We let v_i denote the spectral weight of the mode Ω_i.

First, consider the case of axial symmetry where the relaxation rates Γ_l are small compared to a_1 and a_2. The modes and their spectral weights are given approximately by the equations

$$\Omega_1=\tfrac{3}{2}\omega_d(3z^2-1)\epsilon+\tfrac{2}{3}ia_+^2\Gamma_2\,,$$
$$v_1=a_-^2/3\,,$$
$$\Omega_{2,3}=-\tfrac{3}{4}\omega_d(3z^2-1)\epsilon\mp\omega_c z+i\tfrac{1}{2}(\Gamma_1+\tfrac{1}{3}\Gamma_2 a_-^2)\,, \qquad (20)$$
$$v_{2,3}=a_+^2/3\,,$$

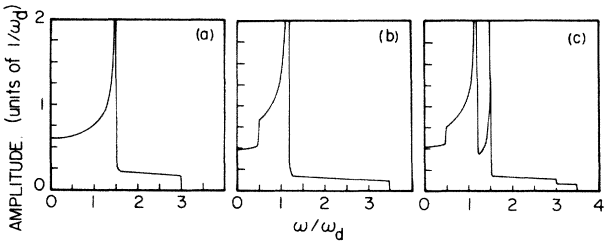

FIG. 1. The line shapes in the case of axial symmetry with very little relaxation. Case (a) corresponds to $m_j=0$, while case (b) corresponds to $m_j=\pm1$. Case (c) is the composite that would be seen if all of the m_j states were equally populated.

where, as discussed in the Appendix, there is a set of modes with $\epsilon=1$ and a set with $\epsilon=-1$. In the limit where the damping can be ignored, a hydrogen molecule can be in states with $m_j=0,\pm1$ and the three different frequencies correspond to nuclear-spin systems feeling each of three different static fields. (The reason for the two sets of three modes is that there are two distinct frequencies corresponding to $\Delta m_1=\pm1$. Equivalently, the line shape consists of the spectrum of the operator B_{11} and the modes correspond to the operator combinations $B_{11}+\epsilon B_{21}$.) The frequencies of the three modes are independent of temperature because a given H_2 molecule is restricted to a state of fixed m_j. We note, however, that the v_i and decay rates are temperature dependent and reflect the fraction of the time spent in a state m_j. Figure 1(a) is the angular averaged spectrum from Ω_1, while Fig. 1(b) is the spectrum from Ω_2 or Ω_3. Figure 1(c) is the sum of the spectra from Ω_1, Ω_2, and Ω_3 with equal weighting. In Ref. 13 only the spectrum of Ω_1 or $\Omega_{2,3}$ alone is considered and, to our knowledge, no spectrum like that in Fig. 1(b) or 1(c) has ever been observed. Figure 1(a), of course, is the familiar Pake doublet.

Next, consider the opposite limiting case of axial symmetry where the relaxation rates are large compared to a_1 and a_2. In this case all of the spectral weight is in one mode with a frequency

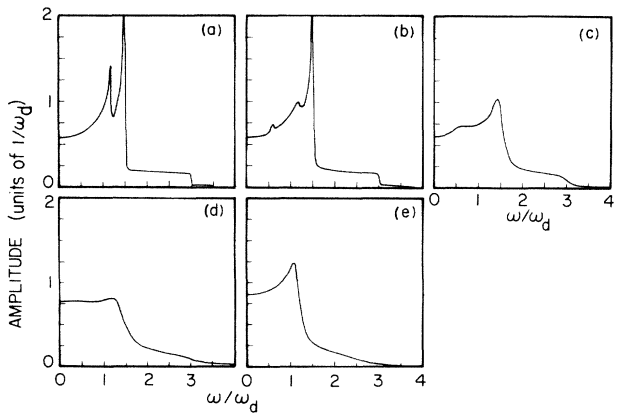

FIG. 2. Spectra for the case of axial symmetry with $a=-\frac{3}{2}$. The values of Γ_2/ω_d are 0.01, 0.1, 1.0, 3.0, and 10.0 for panels (a), (b), (c), (d), and (e), respectively.

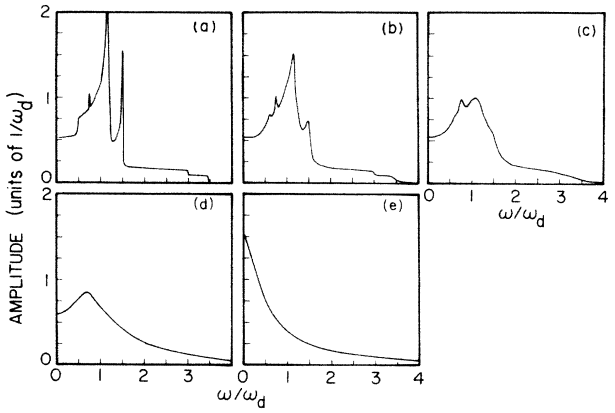

FIG. 3. Spectra for the case of axial symmetry with $a=0$. The values of Γ_2/ω_d are 0.01, 0.1, 0.3, 1.0, and 3.0 for panels (a), (b), (c), (d), and (e), respectively.

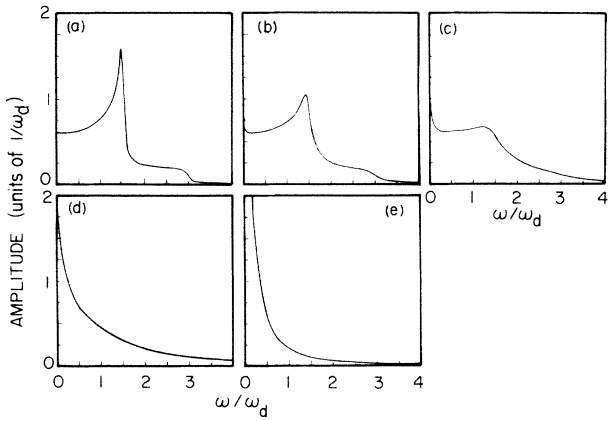

FIG. 5. Spectra for the case of no symmetry with $a=0$. The values of Γ_2/ω_d are 0.1, 0.3, 1.0, 3.0, and 10.0 for panels (a), (b), (c), (d), and (e), respectively.

$$\Omega=-[\tfrac{3}{4}\omega_d(3z^2-1)a\epsilon+i(\tfrac{2}{3}\omega_c^2a_+^2/\Gamma_1)+i\tfrac{9}{8}\omega_d^2(3z^2-1)^2a_+^2a_-^2/\Gamma_b]\ . \tag{21}$$

The line shape is, of course, a simple Lorentzian. In this case a given H_2 molecule is flipping quite rapidly between states of different m_j and thus the H_2 nucleus sees an average field which is temperature dependent because the weighting of the different states is temperature dependent. There is additional temperature dependence in the decay rate (besides the temperature dependence of Γ_1 and Γ_2) for the same reason.

The transition between the two limiting cases is shown in Figs. 2–4 for three different values of a. As can be seen, the two-peaked structure evolves into the Pake doublet. We wish to particularly note the apparent glitches in some of the spectra at $\omega\simeq 0.75\omega_d$ and a weaker one at $\omega\simeq 0.6\omega_d$. The first one occurs from the part of the angular average near $z=0$ where a_1 is zero and where two of the modes (Ω_2 and Ω_3) become degenerate. The second glitch comes from values of z where $\Omega_1\simeq\Omega_2$ or Ω_3. An analysis of the modes near these points shows that the two modes stay degenerate to first order in $z-z_0$ near the point of degeneracy, which is $z=z_0$. This quadratic dependence on $z-z_0$ causes the glitch. The width and amplitude of the glitches are very dependent on Γ_a, becoming much weaker as Γ_a increases.

For the case of no symmetry we first consider the limit where the relaxation rate Γ_2 is small compared to a_1 and a_2. The modes and spectral weight functions are given by the equations

$$\begin{aligned}
&\Omega_1=\tfrac{3}{2}\omega_d(3z^2-1)\epsilon+i\tfrac{2}{3}\Gamma_2a_+^2\ ,\\
&v_1=a_-^2/3\ ,\\
&\Omega_{2,3}=[-\tfrac{3}{4}(3z^2-1)\mp(1-z^2)\cos\phi]\omega_d\epsilon\\
&\qquad+i\tfrac{1}{2}(1+\tfrac{1}{3}a_-^2)\Gamma_2\ ,\\
&v_{2,3}=a_+^2/3\ .
\end{aligned} \tag{22}$$

In the limit where the damping can be ignored, each of these Ω_i gives the same Pake doublet when averaged over

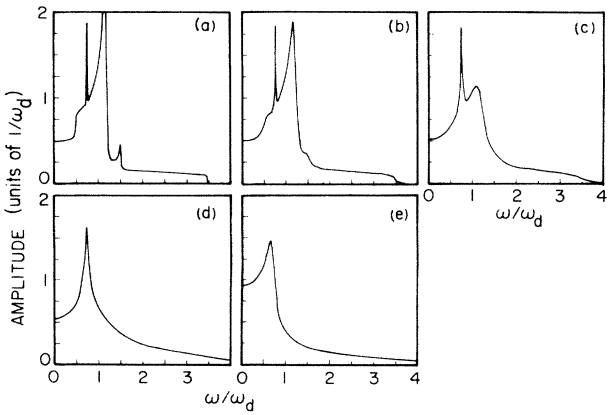

FIG. 4. Spectra for the case of axial symmetry with $a=\frac{3}{4}$. The values of Γ_2/ω_d are 0.01, 0.1, 0.3, 1.0, and 3.0 for panels (a), (b), (c), (d), and (e), respectively.

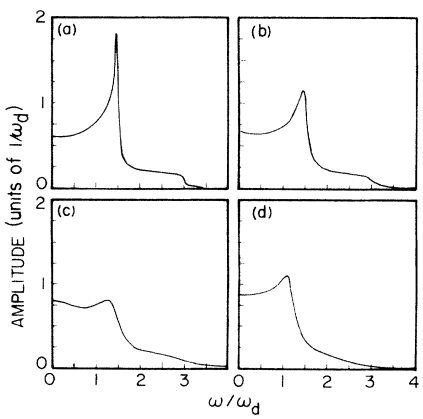

FIG. 6. Spectra for the case of no symmetry with $a=-\frac{3}{2}$. The values of Γ_2/ω_d are 0.3, 1.0, 3.0, and 10.0 for panels (a), (b), (c), and (d), respectively.

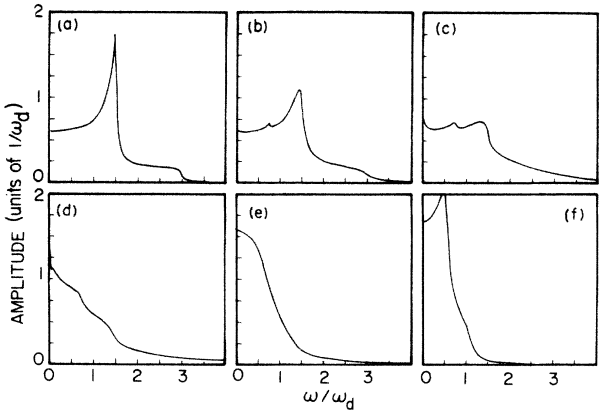

FIG. 7. Spectra for the case of no symmetry with $a=\frac{3}{4}$. The values of Γ_2/ω_d are 0.1, 0.3, 1.0, 3.0, 10.0, and 30.0 for panels (a), (b), (c), (d), (e), and (f), respectively.

all angles. Most of the discussion following Eqs. (20) is also valid here.

Finally, we consider the case of no symmetry where the relaxation rate Γ_2 is large compared to a_1 and a_2. In this case all of the spectral weight is in one mode with a frequency

$$\Omega=\tfrac{3}{4}(3z^2-1)a\omega_d\epsilon + \tfrac{3}{2}ia_+^2[(\tfrac{3}{2})^2(1-z^2)^2\cos^2\phi + \tfrac{3}{4}(3z^2-1)^2a_-^2]\omega_d^2/\Gamma_2 , \quad (23)$$

and the discussion following Eq. (21) is valid here also.

The transition region between these two limiting cases is shown in Figs. 5–7 for three different values of a. Again there is an apparent glitch, this time at $\omega=0$. This little spike is considerably weaker than in the case of axial symmetry. One can obtain quasianalytic forms for this glitch by expanding about the point $z^2=\frac{1}{3}$ and $\cos\psi=0$. Again, its width and amplitude depend critically on Γ_a.

Although the equations in the paper have been derived for an isolated H_2 molecule, most aspects of our results do not depend very heavily on this assumption. That is, the relaxation rates and $\langle A_{20}\rangle$ are input for the calculations and they could have been determined by *EQQ* interactions. Thus the glitch observed[14–16] in the line shape of concentrated H_2 could easily be related to the one discussed here.

Finally, we wish to note that the case of axial symmetry gives Pake doublets with splittings of about $3\omega_d$ and about $3\omega_d/2$ under a fairly wide variety of conditions. The no-symmetry case does not include the doublet at $3\omega_d/2$. Since this latter doublet does not appear to have been observed, one must wonder if the conditions of axial symmetry have ever been observed.

ACKNOWLEDGMENTS

This work was supported in part by the National Science Foundation under Grant No. DMR-85-03083.

APPENDIX

The nonzero elements of the matrix $M_{\alpha\beta}$ in Eq. (7) are

$$\begin{aligned}
&M_{14}=M_{41}=3a_2a\ ,\quad M_{12}=M_{21}=\tfrac{3}{2}^{1/2}a_1a_+\ ,\\
&M_{16}=M_{61}=3a_2a_+a_-/2^{1/2}\ ,\quad M_{15}=M_{51}=3^{1/2}a_1a_-/2\ ,\\
&M_{23}=M_{32}=3^{1/2}a_1a_-/2\ ,\\
&M_{36}=M_{63}=-3a_2(1+2a)/2\ ,\\
&M_{34}=M_{43}=3a_1a_+a_-/2^{1/2}\ ,\quad M_{45}=M_{54}=\tfrac{3}{2}^{1/2}a_1a_+\ ,\\
&M_{56}=M_{65}+3^{1/2}a_1a_+/2\ ,\\
&M_{11}=\omega+i\Gamma_{1a}\ ,\quad M_{22}=\omega+i\Gamma_{2a}\ ,\quad M_{33}=\omega+i\Gamma_1\ ,\\
&M_{44}=\omega+i\Gamma_2\ ,\quad M_{55}=\omega+i\Gamma_1\ ,\quad M_{66}=\omega+i\Gamma_2\ .
\end{aligned} \quad (A1)$$

The operators p_α for the case of axial symmetry are given by the equations

$$\begin{aligned}
&p_1=B_{11}\ ,\quad p_2=B_{11}A_{10}\ ,\quad p_3=B_{11}\tilde{A}_{20}/A\ ,\\
&p_4=B_{21}\ ,\quad p_5=B_{21}A_{10}\ ,\quad p_6=B_{21}\tilde{A}_{20}/A\ ,
\end{aligned} \quad (A2)$$

where

$$A^2=[\mathrm{tr}(\tilde{A}_{20})^2]^{1/2}=a_+a_-\ . \quad (A3)$$

The operators for the case of no symmetry are

$$\begin{aligned}
&p_1=B_{11}\ ,\quad p_2=B_{11}A_{b0}\ ,\quad p_3=B_{11}\tilde{A}_{20}/A\ ,\\
&p_4=B_{21}\ ,\quad p_5=B_{21}A_{b0}\ ,\quad p_6=B_{21}\tilde{A}_{20}/A\ .
\end{aligned} \quad (A4)$$

If $\Gamma_{a1}=\Gamma_{a2}=\Gamma_a$, then the 6×6 matrix M decomposes into a direct product of two 3×3 matrices, $N_{ij}(\epsilon)$, where $\epsilon=\pm1$ and

$$\begin{aligned}
&N_{11}(\epsilon)=\omega+i\Gamma_a+3\epsilon a_2a\ ,\quad N_{22}(\epsilon)=\omega+i\Gamma_1+3\epsilon a_2/2\ ,\\
&N_{33}(\epsilon)=\omega+i\Gamma_2-3\epsilon a_2(1+a)/2\ ,\\
&N_{12}(\epsilon)=N_{21}(\epsilon)=\tfrac{3}{2}^{1/2}a_1a_+\ ,\\
&N_{13}(\epsilon)=n_{31}(\epsilon)=3\epsilon a_2a_+a_-/2^{1/2}\ ,\\
&N_{23}(\epsilon)=n_{32}(\epsilon)=3^{1/2}a_1a_-/2\ .
\end{aligned} \quad (A5)$$

These matrices solve the equation

$$N_{ij}(\epsilon)Q_j(\epsilon)=0\ ,$$

where

$$Q_1(\epsilon)=p_1+\epsilon p_4\ ,Q_2(\epsilon)=p_2+\epsilon p_5\ ,Q_3(\epsilon)=p_3+\epsilon p_6\ .$$

[1]P. A. Fedders, Phys. Rev. B 20, 2588 (1979).
[2]P. A. Fedders, Phys. Rev. B 30, 3603 (1984).
[3]M. S. Conradi, K. Luszczynski, and R. E. Norberg, Phys. Rev. B 20, 2594 (1979).
[4]R. F. Buzerak, M. Chan, and H. Meyer, Solid State Commun. 18, 685 (1976).
[5]J. R. Gaines, Y. C. Shi, and J. H. Constable, Phys. Rev. B 17, 102 (1978).

[6]R. E. Norberg, Phys. Rev. B **31**, 7925 (1985).
[7]J. B. Boyce and M. Stutzmann, Phys. Rev. Lett. **54**, 562 (1985).
[8]F. Reif and E. M. Purcell, Phys. Rev. **91**, 631 (1953).
[9]M. Bloom, I. Oppenheim, M. Lipsicas, C. G. Wade, and C. Yarnell, J. Chem. Phys. **43**, 1036 (1965).
[10]P. A. Fedders, Phys. Rev. B **10**, 4510 (1974).
[11]D. J. Leopold, J. B. Boyce, P. A. Fedders, and R. E. Norberg, Phys. Rev. B **26**, 6053 (1982).
[12]J. Van Kranendonk and M. B. Walker, Can. J. Phys. **46**, 2441 (1968).
[13]N. S. Sullivan, M. Devoret, B. P. Cowan, and C. Urbina, Phys. Rev. B **17**, 5016 (1978).
[14]D. Esteve, M. Devoret, and N. S. Sullivan, J. Phys. C **15**, 5455 (1982).
[15]S. Washburn, M. Calkins, H. Meyer, and A. B. Harris, J. Low. Temp. Phys. **49**, 101 (1982).
[16]H. Meyer and S. Washburn, J. Low Temp. Phys. **57**, 31 (1983).